Laser-ablation assisted strain engineering of gold nanoparticles for selective electrochemical CO_2 reduction

Chao Zhang[a‡], Wei Zhang[e‡], Ferdi Karadas[d], Jingxiang Low[b], Ran Long[b], Changhao Liang[c*], Jin Wang[a], Zhengquan Li[a*], Yujie Xiong[b*]

[a]*Key Laboratory of the Ministry of Education for Advanced Catalysis Materials, Zhejiang Normal University, Jinhua, Zhejiang 321004, China*

[b]*School of Chemistry and Materials Science, University of Science and Technology of China, Hefei 230026, China*

[c]*Key Laboratory of Materials Physics and Anhui Key Laboratory of Nanomaterials and Nanotechnology, Institute of Solid State Physics, Chinese Academy of Sciences, Hefei 230031, China*

[d]*National Nanotechnology Research Center, and Department of Chemistry, Bilkent University, 06800 Ankara, Turkey*

[e]*Institute for Energy Research, Jiangsu Unversity, Zhenjiang, Jiangsu 212013, China*

E-mail: chliang@issp.ac.cn, zqli@zjnu.edu.cn, yjxiong@ustc.edu.cn

‡These authors contributed equally to this work.

***In situ* Raman spectroscopy measurements**

For the *in situ* Raman spectroscopy measurements, all of the measurements were performed on a WITec alpha 300R confocal Raman microscope with a 600 grooves/mm diffraction grating. A 532 nm excitation laser with a power of 5 mW was used as excitation source. Calibration was conducted based on the peak at 520 cm^{-1} of a silicon wafer standard. An H-shape cell separated by an anion exchange membrane was employed to perform *in situ* Raman spectroscopy characterization for electrochemical CO_2 reduction (Figure R1). An Ag/AgCl (saturated with KCl) electrode and a Pt wire were used as the reference and counter electrodes, respectively. Before the test, 0.1 M $KHCO_3$ was purged with high-purity CO_2 gas for 30 min and then added into the H-shape cell. The electrocatalytic process was studied via a CHI 660E electrochemical workstation, and *in situ* Raman spectra were obtained under potentiostatic conditions.

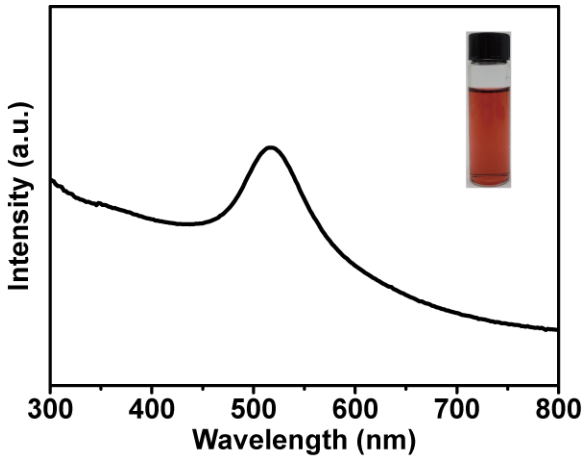

Fig. S1 UV-vis absorption spectrum of Au-LAL colloids and (inset) photograph of Au-LAL colloids.

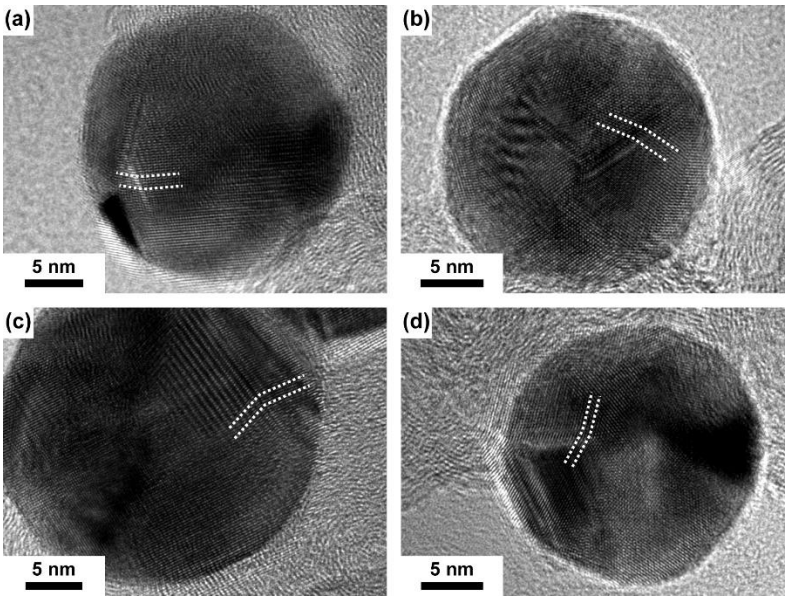

Fig. S2 TEM images of the Au-LAL, taken from four randomly-selected nanoparticles.

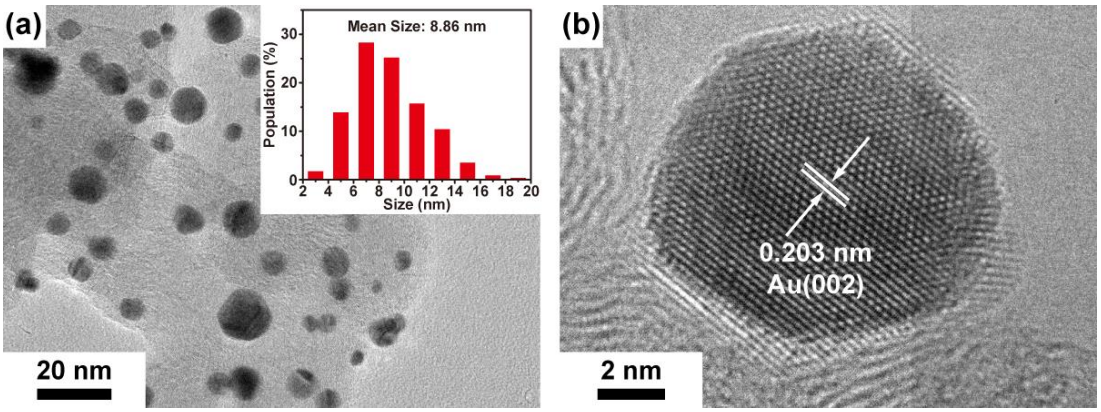

Fig. S3 (a) TEM image of Au-A NPs and (inset) the size distribution of Au-A NPs. (b) HRTEM image of an Au-A nanoparticle.

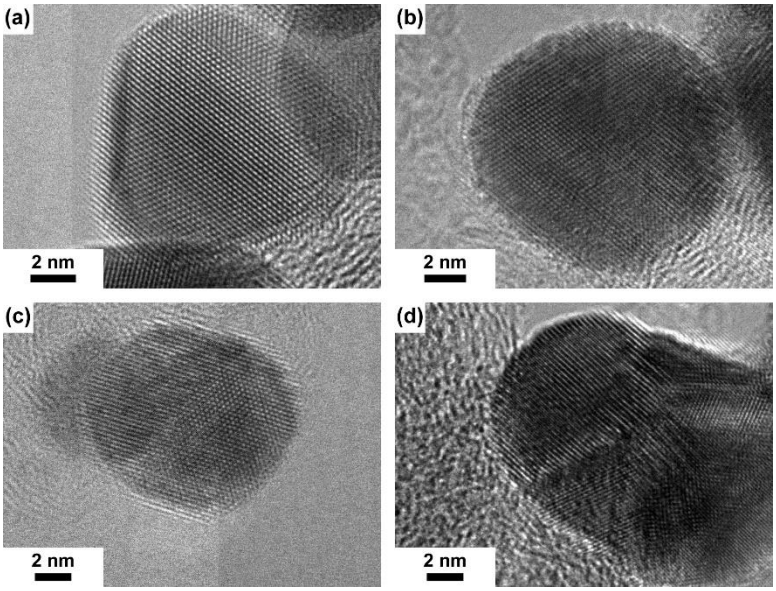

Fig. S4 TEM images of the Au-A, taken from four randomly-selected nanoparticles.

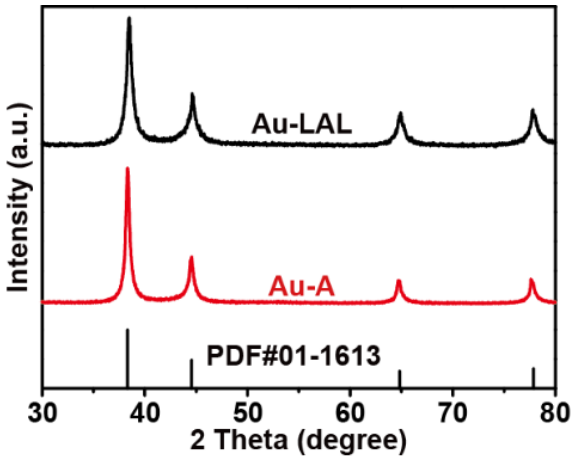

Fig. S5 XRD patterns of Au-LAL and Au-A.

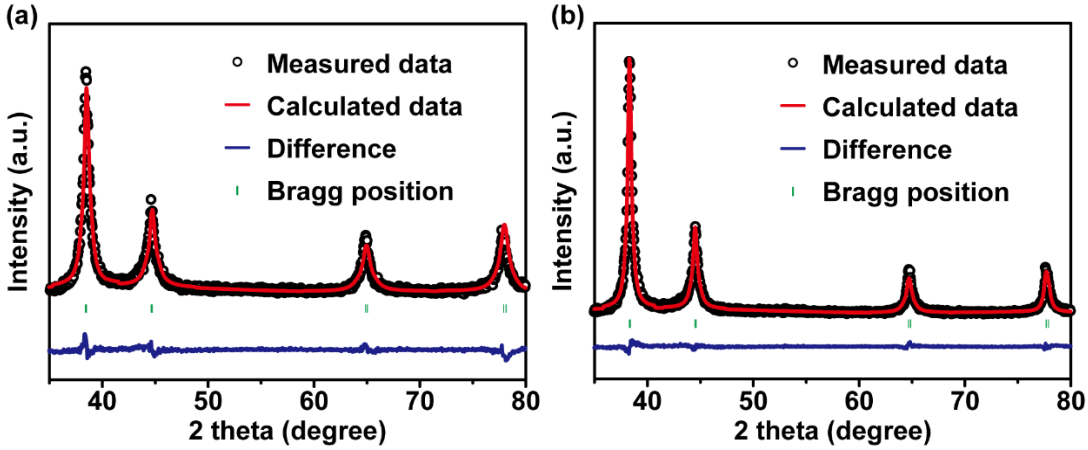

Fig. S6 Rietveld refined XRD patterns of (a) Au-LAL and (b) Au-A.

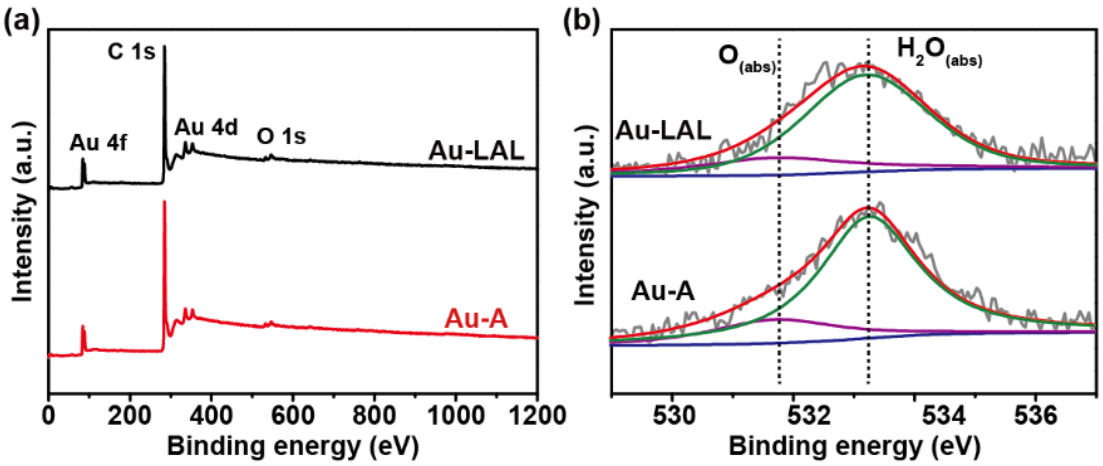

Fig. S7 (a) The survey XPS spectra and (b) high-resolution O 1s XPS spectra of Au-LAL and Au-A.

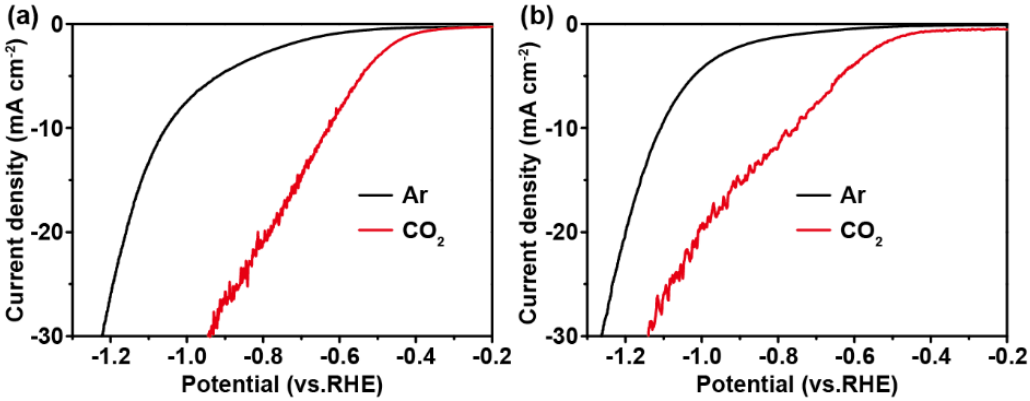

Fig. S8 The LSV curves of (a) Au-LAL and (b) Au-A in Ar and CO_2-saturated 0.1 M $KHCO_3$ electrolyte.

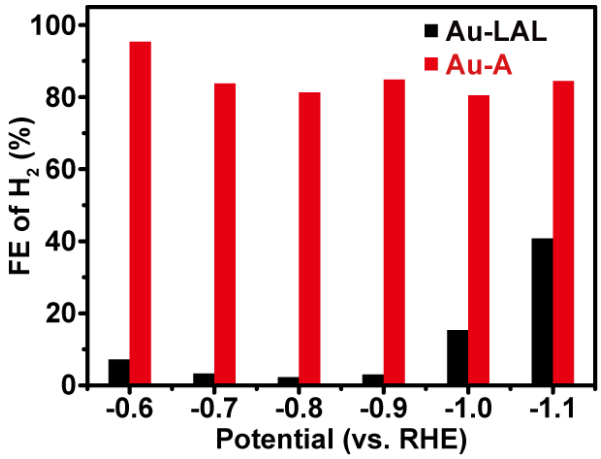

Fig. S9 The Faraday efficiencies (FEs) of H_2 for Au-LAL and Au-A NPs.

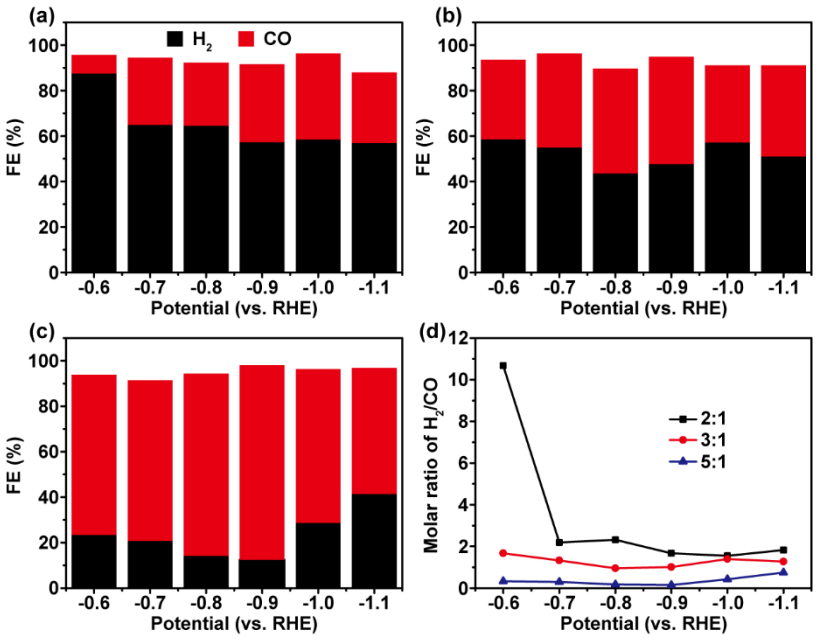

Fig. S10 FEs of CO and H_2 at different applied potentials for Au-LAL and Au-A with different mass ratio of (a) 2:1, (b) 3:1 and (c) 5:1. (d) Molar ratio of H_2/CO for Au-LAL and Au-A with different mass ratio.

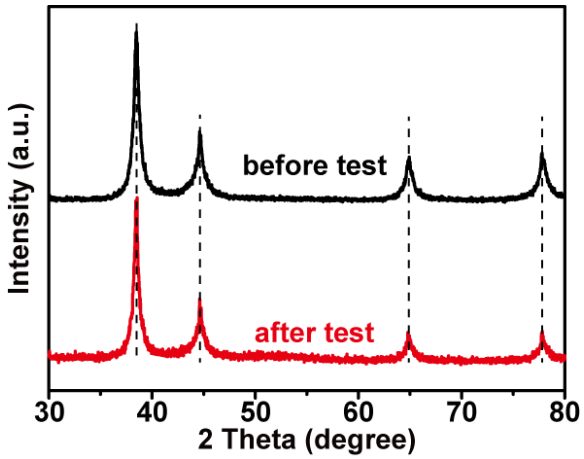

Fig. S11 XRD patterns of Au-LAL NPs before and after electrochemical CO_2 reduction stability test.

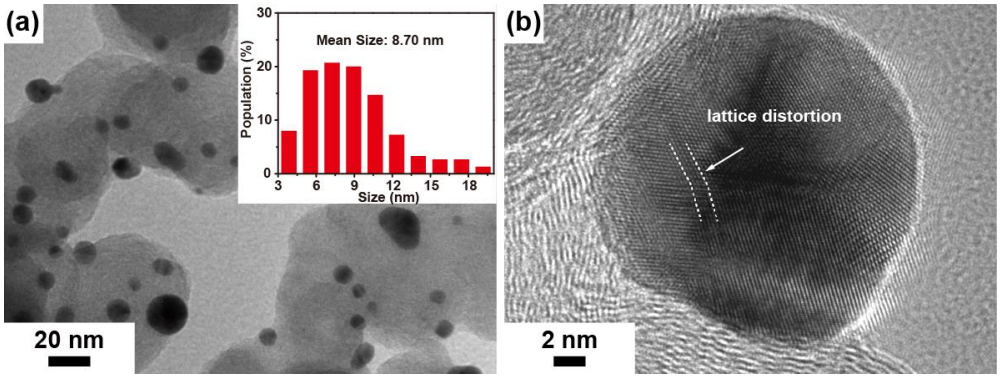

Fig. S12 (a) TEM and (b) HRTEM images of Au-LAL after stability test. The inset shows the size distribution of Au-LAL after the stability test.

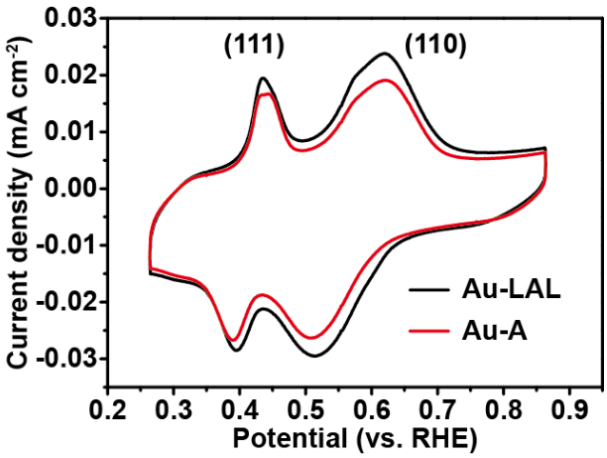

Fig. S13 Pb-UPD CV curves of Au-LAL and Au-A.

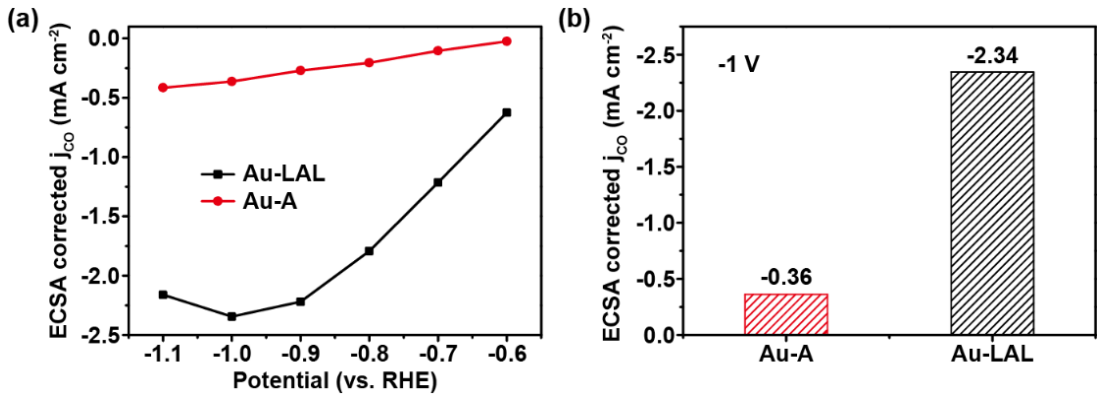

Fig. S14 (a) ECSA-corrected CO partial current density and (b) ECSA-corrected CO partial current density at −1 V of Au-LAL and Au-A.

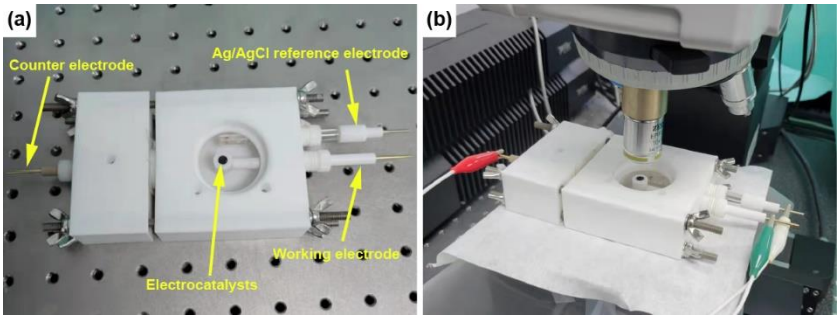

Figure S15. (a) The electrochemical cell and (b) the experimental setup for *in situ* Raman spectroscopy measurements.

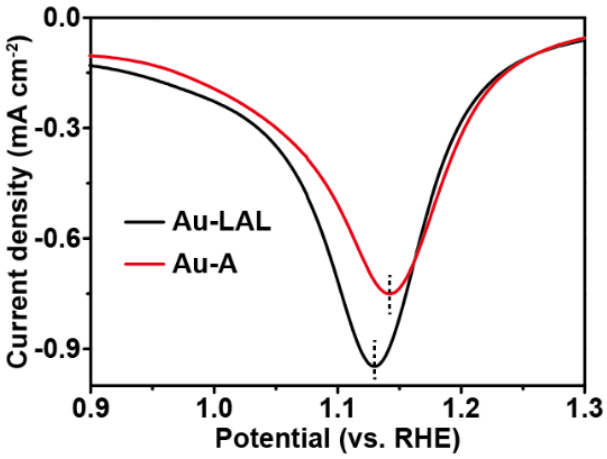

Fig. S16. The magnified region from 1.3 to 0.9 V of cyclic voltammograms for Au-LAL and Au-A in Ar-saturated 0.1 M $HClO_4$ electrolyte with a scan rate of 20 mV s^{-1}.

Table S1. The FEs of electrochemical CO_2 reduction products (H_2 and CO) for Au-LAL and Au-A NPs.

Sample	Potential (V)	−0.6	−0.7	−0.8	−0.9	−1.0	−1.1
Au-LAL	FEs of H_2 (%)	7.2	3.3	2.3	2.8	15.3	40.8
	FEs of CO (%)	85.1	93.3	95.8	97	81.2	58
	j_{CO} (mA cm^{-2})	−7	−13.6	−20.1	−24.9	−26.3	−24.2
Au-A	FEs of H_2 (%)	95.4	83.8	81.3	84.9	80.5	84.5
	FEs of CO (%)	4.1	10.7	15.8	16.2	18	16.7
	j_{CO} (mA cm^{-2})	−0.25	−1.06	−2.1	−2.77	−3.7	−4.24

Table S2. Comparation of Au-based electrocatalysts toward electrochemical CO_2 reduction.

Electrocatalysts	Electrolyte	Highest FEs (V RHE)	j_{CO} with highest FEs in H-cell (mA cm^{-2})	Reference
Au-LAL	0.1 M $KHCO_3$	97% at −0.9 V	24.7	This work
Au-CDots-C_3N_4	0.5 M $KHCO_3$	79.8% at −0.5 V	below 5	1
Au-CeO_x/C	0.1 M $KHCO_3$	89.1% at −0.89 V	12.9	2
De-Au_3Cu	0.5 M $KHCO_3$	94.3% at −0.43 V	\	3
4H-Au nanoribbons	0.1 M $KHCO_3$	90% at −0.7 V	6.2	4
nanoporous Au	0.5 M $KHCO_3$	94% at −0.6 V	\	5
o-$AuCu_3$@fct Au	0.1 M $KHCO_3$	94.5% at −0.8 V	\	6
Pd_1Au_{24} nanoclusters	0.1 M $KHCO_3$	∼100% at −0.9 V	20.3	7
$Au_{19}Cd_2$ nanoclusters	0.5 M $KHCO_3$	95% at −0.9 V	40	8
Mo-doped Au NPs	0.5 M $KHCO_3$	97.5% at −0.4 V	11.22	9
Au−MPA/C	0.5 M $KHCO_3$	96.2% at −0.75 V	19.2	10
ER-Au-UR/C	0.1 M $KHCO_3$	94.2% at −0.68 V	9.4	11
nanoporous Au_3Cu	0.1 M $KHCO_3$	∼100% at −0.7 V	below 25	12
pc-NPG	0.5 M $KHCO_3$	98% at −0.5 V	11.8	13
Au aerogel	0.1 M $KHCO_3$	95.6% at −0.5 V	4.78	14
AuCu aerogel	0.1 M $KHCO_3$	92% at −0.7 V	7.42	15
AuPd aerogel	0.1 M $KHCO_3$	99.96% at −0.5 V	2.4	16

Table S3. The FEs of CO_2 reduction products (H_2 and CO) for Au-LAL and Au-A with different mass ratio.

Sample	Potential (V)	−0.6	−0.7	−0.8	−0.9	−1.0	−1.1
2:1	FEs of H_2 (%)	87.5	64.9	264.5	57.3	58.5	56.9
	FEs of CO (%)	8.2	29.6	27.8	34.3	37.8	31.1
3:1	FEs of H_2 (%)	58.6	54.9	43.6	47.7	57.2	51.1
	FEs of CO (%)	35	41.4	46	47.1	40.9	40
5:1	FEs of H_2 (%)	23.4	20.8	14.2	12.5	28.7	41.4
	FEs of CO (%)	70.4	70.7	80.1	85.6	67.6	55.5

Table S4. ECSA-corrected CO partial current density of Au-LAL and Au-A NPs.

Potential (V)	−0.6	−0.7	−0.8	−0.9	−1.0	−1.1
Au-LAL (mA cm^{-2})	−0.62	−1.21	−1.79	−2.22	−2.34	−2.16
Au-A (mA cm^{-2})	−0.02	−0.10	−0.21	−0.27	−0.36	−0.42

Table S5. The adsorption free energy (eV) of CO_2 electroreduction adsorption species for normal and strained Au NPs.

Sample	CO_2(g) /eV	*CO_2 /eV	*COOH /eV	*CO + H_2O(g) /eV	CO(g) + H_2O(g) /eV	Barrier energy /eV
Strained Au	1.407	1.168	2.211	2.053	1.865	1.043
Normal Au	1.407	1.824	2.982	2.531	1.865	1.158

Table S6. The ZPE and TS for adsorption species for normal and strained Au NPs.

Sample	$*CO_2$		*COOH		$*CO+H_2O(g)$	
	ZPE/(eV)	-TS/(eV)	ZPE/(eV)	-TS/(eV)	ZPE/(eV)	-TS/(eV)
Strained Au	0.308	0.137	0.616	0.173	0.793	0.126
Normal Au	0.305	0.074	0.623	0.153	0.809	0.104

Reference

1. H. Dong, L. Zhang, L. L. Li, W. Deng, C. L. Hu, Z. J. Zhao and J. L. Gong, *Small*, 2019, **15**, 1900289.

2. D. Gao, Y. Zhang, Z. Zhou, F. Cai, X. Zhao, W. Huang, Y. Li, J. Zhu, P. Liu, F. Yang, G. Wang and X. Bao, *J. Am. Chem. Soc.*, 2017, **139**, 5652–5655.

3. W. Zhu, L. Zhang, P. Yang, C. Hu, H. Dong, Z. J. Zhao, R. Mu and J. Gong, *ACS Energy Lett.*, 2018, **3**, 2144–2149.

4. Y. Wang, C. Y. Li, Z. X. Fan, Y. Chen, X. Li, L. Cao, C. H. Wang, L. Wang, D. Su, H. Zhang, T. Mueller and C. Wang, *Nano Lett.*, 2020, **20**, 8074–8080.

5. W. Q. Zhang, J. He, S. Y. Liu, W. X. Niu, P. Liu, Y. Zhao, F. J. Pang, W. Xi, M. W. Chen, W. Zhang, S. S. Pang and Y. Ding, *Nanoscale*, 2018, **10**, 8372–8376.

6. D. Yu, L. Gao, T. Sun, J. Guo, Y. Yuan, J. Zhang, M. Li, X. X. Li, M. C. Liu, C. Ma, Q. H. Liu, A. L. Pan, J. L. Yang and H. W. Huang, *Nano Lett.*, 2021, **21**, 1003–1010.

7. S. Li, D. Alfonso, A. V. Nagarajan, S. D. House, J. C. Yang, D. R. Kauffman, G. Mpourmpakis and R. C. Jin, *ACS Catal.*, 2020, **10**, 12011–12016.

8. S. Li, A. V. Nagarajan, D. R. Alfonso, M. Sun, D. R. Kauffman, G. Mpourmpakis and R. C. Jin, *Angew. Chem. Int. Ed.*, 2021, **60**, 6351–635.

9. K. Sun, Y. Ji, Y. Liu and Z. Wang, *J. Mater. Chem. A*, 2020, **8**, 12291–12295.

10. Z. Zhuang, Y. Zhang, L. Hu, H. Ying and W. Q. Han, *Chem. Asian J.*, 2020, **15**, 2153–2159.

11. Y. Zhang, L. Hu and W. Han, *J. Mater. Chem. A*, 2018, **6**, 23610–23620.

12. X. Ma, Y. Shen, S. Yao, M. Shu, R. Si and C. H. An, *Chem. Eur.J.*, 2020, **26**, 4143–

4149.

13. X. L. Lu, T. S. Yu, H. L. Wang, L. H. Qian and P. X. Lei, *ACS Catal.*, 2020, **10**, 8860–8869.

14. S. Yan, S. A. Mahyoub, J. Lin, C. Zhang, Q. Hu, C. Z. Chen, F. Zhang and Z. Cheng, *Nanotechnology*, 2022, **33**, 125705.

15. D. Z. Zhong, L. Zhang, Q. Zhao, D. F. Cheng, W. Y. Deng, B. Liu, G. Zhang, H. Dong, X. T. Yuan, Z. Zhao, J. P. Li and J. L. Gong, *J. Chem. Phys.*, 2020, **152**, 204703.

16. R. Du, W. Jin, H. Wu, R. Hübner, L. Zhou, G. Xue, Y. Hu and A. Eychmüller, *J. Mater. Chem. A*, 2021, **9**, 17189–17197.